Neurogenetics (2010) 11:53–71
DOI 10.1007/s10048-009-0203-3

ORIGINAL ARTICLE

A modifier locus on chromosome 5 contributes to *L1 cell adhesion molecule* X-linked hydrocephalus in mice

Alexis Tapanes-Castillo · Eli J. Weaver · Robin P. Smith · Yoshimasa Kamei · Tamara Caspary · Kara L. Hamilton-Nelson · Susan H. Slifer · Eden R. Martin · John L. Bixby · Vance P. Lemmon

Received: 6 April 2009 / Accepted: 8 June 2009 / Published online: 30 June 2009

Abstract Humans with *L1 cell adhesion molecule* (*L1CAM*) mutations exhibit X-linked hydrocephalus, as well as other severe neurological disorders. *L1-6D* mutant mice, which are homozygous for a deletion that removes the sixth immunoglobulin-like domain of *L1cam*, seldom display hydrocephalus on the 129/Sv background. However, the same *L1-6D* mutation produces severe hydrocephalus on the C57BL/6J background. To begin to understand how *L1cam* deficiencies result in hydrocephalus and to identify modifier loci that contribute to X-linked hydrocephalus by genetically interacting with *L1cam*, we conducted a genome-wide scan on F2 *L1-6D* mice, bred from *L1-6D* 129S2/SvPasCrlf and C57BL/6J mice. Linkage studies, utilizing chi-square tests and quantitative trait loci mapping techniques, were performed. Candidate modifier loci were further investigated in an extension study. Linkage was confirmed for a locus on chromosome 5, which we named *L1cam hydrocephalus modifier 1* (*L1hydro1*), $p = 4.04 \times 10^{-11}$.

Keywords *L1cam* · Hydrocephalus · Modifier · Linkage analysis · QTL

Electronic supplementary material The online version of this article (doi:10.1007/s10048-009-0203-3) contains supplementary material, which is available to authorized users.

A. Tapanes-Castillo · E. J. Weaver · R. P. Smith · J. L. Bixby · V. P. Lemmon (✉)
The Miami Project to Cure Paralysis,
Miller School of Medicine, University of Miami,
Lois Pope LIFE Center, Room 4-16, 1095 NW 14th Terrace,
Miami, FL 33136, USA
e-mail: vlemmon@miami.edu

E. J. Weaver · Y. Kamei · V. P. Lemmon
Department of Neuroscience, Case Western Reserve University,
Cleveland, OH, USA

R. P. Smith · J. L. Bixby · V. P. Lemmon
Neuroscience Program, University of Miami,
Miami, FL, USA

T. Caspary
Department of Human Genetics, Emory University,
Atlanta, GA, USA

K. L. Hamilton-Nelson · S. H. Slifer · E. R. Martin
Dr. John T. MacDonald Foundation,
Department of Human Genetics,
Miami Institute for Human Genomics, University of Miami,
Miami, FL, USA

J. L. Bixby · V. P. Lemmon
Department of Neurological Surgery, Miller School of Medicine,
University of Miami,
Miami, FL, USA

J. L. Bixby
Department of Molecular and Cellular Pharmacology,
Miller School of Medicine, University of Miami,
Miami, FL, USA

Present Address:
Y. Kamei
Department of Maternal, Fetal and Neonatal Medicine,
University of Tokyo Hospital,
Tokyo, Japan

Introduction

Hydrocephalus is a devastating neurological condition, characterized by the abnormal accumulation of cerebrospinal fluid (CSF) within the cerebral ventricles. Ineffective treatment can lead to cerebral atrophy and death. Human hydrocephalus is categorized based on two criteria: (1) time of onset and (2) type of CSF flow defect. Depending on the time of onset, hydrocephalus is classified as congenital or acquired. Congenital hydrocephalus arises prenatally, and it occurs with an estimated incidence of 1 in 1,500 births [1, 2]. Acquired hydrocephalus, which develops during or after birth, may be caused by infectious diseases, traumatic brain injuries, or tumors. In addition, hydrocephalus is classified as communicating (non-obstructive) or non-communicating (obstructive) based on the reason for the defect in CSF flow. Communicating hydrocephalus arises from problems with CSF secretion or resorption; CSF flows freely between the ventricles and the subarachnoid space. On the other hand, non-communicating hydrocephalus develops when a physical obstruction blocks CSF flow between the cerebral ventricles and the subarachnoid space.

Linkage analysis of numerous human kindreds with congenital hydrocephalus led to the discovery that mutations in the *L1 cell adhesion molecule* (*L1CAM*) gene are responsible for X-linked hydrocephalus [3], a form of hydrocephalus that has been estimated to account for approximately 7–15% of all congenital hydrocephalus cases [4]. While the autosomal locus 8q12.2-21.2 has also been associated with hydrocephalus [5], additional genes have not been identified. Hence, the molecular etiology of human hydrocephalus is poorly understood.

Fortunately, the use of animal models has provided some insight into the genetics of congenital hydrocephalus. Studies on mutant mice have identified at least 14 genes that cause hydrocephalus when disrupted, including *L1cam*, *metal response transcription factor 2* (*Mtf2*), *platelet-activating factor acetylhydrolase* (*Pafah1b1/Lis1*), *hydrocephalus with hop gait* (*hyh*), and *nuclear factor I-A* ([6–12], reviewed by [13]). Overexpression of *transforming growth factor-β1* has also been shown to cause hydrocephalus in mice [14, 15]. In addition, a quantitative trait loci (QTL) study in mice revealed three loci that regulate cerebral ventricle size [16], and QTL analyses of the Hydrocephalic Texas strain HTX rat led to the mapping of four QTLs that contribute to hydrocephalus [17]. Furthermore, mouse studies demonstrating that hydrocephalus can be caused by mutations in ciliary genes such as *Hydin* and *Dynein axonemal heavy chain 5* (*Mdnah5*) [18–20] have been complemented by data generated from zebrafish. Three genes involved in ciliary function have been associated with the development of hydrocephalus in zebrafish: *polycystin 2*, *fleer*, and *oral-facial-digital type 1 syndrome gene* (*ofd-1*) [21–23].

L1CAM, the only gene currently linked to human hydrocephalus, encodes a Type 1 transmembrane protein that belongs to the immunoglobulin (Ig) superfamily of cell adhesion molecules. The L1 protein consists of six extracellular Ig-like domains, followed by five extracellular fibronectin type III domains, a single transmembrane region, and a cytoplasmic tail. Neuronal L1 is expressed on the surface of axons and growth cones both in the central nervous system (CNS) and in the peripheral nervous system. Schwann cells and other non-neuronal cells, including melanocytes and lymphocytes, also express L1 [24]. L1 mediates cell–cell adhesion, as well as the adhesion of axons to adjacent axons and the extracellular matrix (reviewed in [25]). L1 regulates axon outgrowth (extension and branching), fasciculation, myelination, and neuronal migration [26–31]. L1 has additionally been implicated in synaptic function [32–34].

L1 can function through homo- (L1-L1) or heterophilic interactions [35]. A number of heterophilic binding partners for L1 have been identified, including TAG-1/axonin-1, F3/F11/contactin, phosphacan, neurocan, neuropilin-1, and various integrins (reviewed in [25, 36]). The fibroblast growth factor receptor (FGFR) has also been suggested to directly interact with L1 [37, 38]. Intracellularly, L1 has been shown to signal through Src and mitogen-activated protein kinase 1 (MAPK1/ERK2) and to interact with adaptor molecules such as ezrin, ankyrin, and Ran-binding protein M [39–46].

In humans, mutations in *L1CAM* are responsible for X-linked hydrocephalus, agenesis of the corpus callosum, corticospinal tract hypoplasia, and MASA syndrome—*m*ental retardation, *a*phasia, *s*pastic paraplegia, and *a*dducted thumbs. A comparison of case studies and genetic mutations revealed a striking correlation between the severity of neurological disease and the type of mutation harbored by the *L1CAM* gene [47–49]. Mutations that generate truncations in the extracellular domain of L1 are more likely to be lethal or to produce severe hydrocephalus and grave mental retardation than point mutations in the extracellular domain or mutations that solely affect the cytoplasmic domain. Furthermore, point mutations in the extracellular domain tend to cause more severe neurological problems than cytoplasmic domain mutations.

The severity of hydrocephalus seen in individuals with *L1CAM* mutations is highly variable. Patients range from displaying no hydrocephalus to those having high-pressure progressive hydrocephalus. Aqueductal stenosis is not a constant feature [50–53]. Hence, it has been proposed that individuals carrying *L1CAM* mutations may have communicating hydrocephalus and that observed reductions in the caliber of the aqueduct of Sylvius arise secondarily due to compression from the enlarged ventricles. Intrafamilial

variation has also been observed with respect to *L1CAM*-related hydrocephalus. Differences in the occurrence and severity of hydrocephalus have been documented among related males carrying the same *L1CAM* mutation. For example, within the same family, some males with an *L1CAM* mutation may not exhibit hydrocephalus, while others display moderate or severe hydrocephalus [49–51, 54–57].

L1cam knock-out (*L1KO*) mice bred on a 129/Sv background do not exhibit gross hydrocephalus upon standard pathological examination [6, 7]. However, a subtle, but significant, dilation of the lateral ventricles has been detected with high-resolution magnetic resonance imaging [58]. Interestingly, breeding *L1KO* mice onto a C57BL/6J background enhances the *L1KO* phenotype and results in severe hydrocephalus [6, 48, 59]. This suggests that the degree of ventricular enlargement strongly depends on genetic background, consistent with the intra- and interfamilial variability of hydrocephalus severity in humans. Hence, we hypothesized that ventricle size is regulated by loci that (1) are polymorphic between the 129/Sv and C57BL/6J mouse strains and (2) genetically interact with *L1cam*, to exacerbate the *L1cam* mutant phenotype. Furthermore, we hypothesized that *L1cam* modifier loci could affect hydrocephalus susceptibility and/or severity. Susceptibility modifiers would determine the presence or absence of the phenotype. The same genotype at a susceptibility modifier could exhibit wide variations in severity. In contrast, severity modifiers would affect the magnitude or spectrum of the phenotype. Thus, for a severity modifier to have an effect, the mouse must already be predisposed to hydrocephalus.

In this study, we attempt to uncover the genetic basis of the strain-specific severe hydrocephalus phenotype of *L1cam* mutants. To work toward the identification of *L1cam* modifier genes that contribute to hydrocephalus, we performed genome-wide linkage analyses on hydrocephalic F2 *L1cam* mutants derived from *L1cam* 129S2/SvPasCrlf (129S2) and C57BL/6J mutant mice. Candidate susceptibility loci were detected using chi-square tests to identify markers that deviated from Mendelian segregation in F2 *L1cam* mutants. In addition, QTL analyses of hydrocephalic F2 *L1cam* mutants, as well as chi-square tests comparing mutant mice with moderate versus severe hydrocephalus, were conducted to identify candidate loci that contribute to the severity of the condition.

Materials and methods

Mice and phenotypic analyses

All animal experiments and procedures described in this manuscript were approved by the University of Miami's Institutional Animal Care and Use Committee. To generate *L1cam*$^{tm1.1(L1\text{-}6D)Lem}$ (*L1-6D*) mutant mice, the sixth immunoglobulin-like domain of *L1cam* (exons 12–14) was knocked out using a Cre/lox approach [60]. *L1-6D* heterozygous females (*L1-6D/+)* were then bred to wild-type 129S2/SvPasCrlf (129S2) or C57BL/6J (B6) males for at least 12 generations to generate congenic (Cg) mice. A two-generation, outcross–intercross breeding scheme was next performed to generate the F2 mice utilized for linkage analyses. Briefly, male 129S2.Cg-*L1-6D/Y* and female B6.Cg-*L1-6D/+* mice were bred to produce F1 *L1-6D* 129/B6 mice. The cross was set up in this manner because male and female B6.Cg-*L1-6D* mutants are poor breeders. An intercross was then set up between F1 *L1-6D/Y* males and heterozygous or homozygous F1 *L1-6D* females to generate F2 progeny.

Mice were euthanized with carbon dioxide and evaluated for hydrocephalus postmortem. Hemi- and homozygous 129S2.Cg-*L1-6D* (*N*=36: 32 *L1-6D/Y* males and 4 *L1-6D/L1-6D* females) and B6.Cg-*L1-6D/Y* (*N*=10 males) mice were collected over a wide age-span, ranging from weanlings [postnatal day 21 (p21)] to adults (four B6.Cg-*L1-6D* and eight 129S2.Cg-*L1-6D* mice over 6 months of age). F1 *L1-6D* mutant mice (*N*=16: 14 *L1-6D/Y* males and two *L1-6D/L1-6D* females) were killed between p21 and 3 months of age. All of the F2 mice included in this study were killed p21-p39: wild type (*N*=27: 25 males and two females), *L1-6D/+* (*N*=38 females), and *L1-6D* mutants (*N*=1,058: 540 *L1-6D/Y* males and 518 *L1-6D/L1-6D* females). In particular, 186 of these F2 *L1-6D* mutant mice (105 *L1-6D/Y* males and 81 *L1-6D/L1-6D* females) were killed during a tight window, p21–p30, and utilized for linkage analyses. Once their phenotype was evaluated (as described below), they were divided into two categories: (1) hydrocephalic/affected (*N*=156: 93 males and 63 females) and (2) non-hydrocephalic/unaffected (*N*=30: 12 males and 18 females). Hydrocephalic F2 *L1-6D* mice were further separated into two subgroups: (1) mice that participated in both the genome-wide scan and extension study (*N*=92: 54 males and 38 females) and (2) mice that solely participated in the extension study (*N*=64: 39 males and 25 females).

Whole brains were dissected from animals, rinsed with 1× phosphate buffered saline, and fixed in 4% paraformaldehyde. At least 24-h postfixation, thick coronal sections were prepared. Brains were positioned with the cortical surface parallel to the horizontal plane. A razor blade, placed rostral to the cerebral cortex, was used to secure each brain in place. Meanwhile, approximately four 1-mm sections were cut, perpendicular to the brain surface, along the rostral-caudal axis of the cortex using a scalpel (Bard-Parker no. 371610; Fig. 1a). Sections were then examined under a dissecting microscope (Olympus SZ-40, ×1.5 and Wild Heerbrugg MG50, ×16). Sections were rarely damaged during dissection. Nevertheless, marred samples were not included in the study.

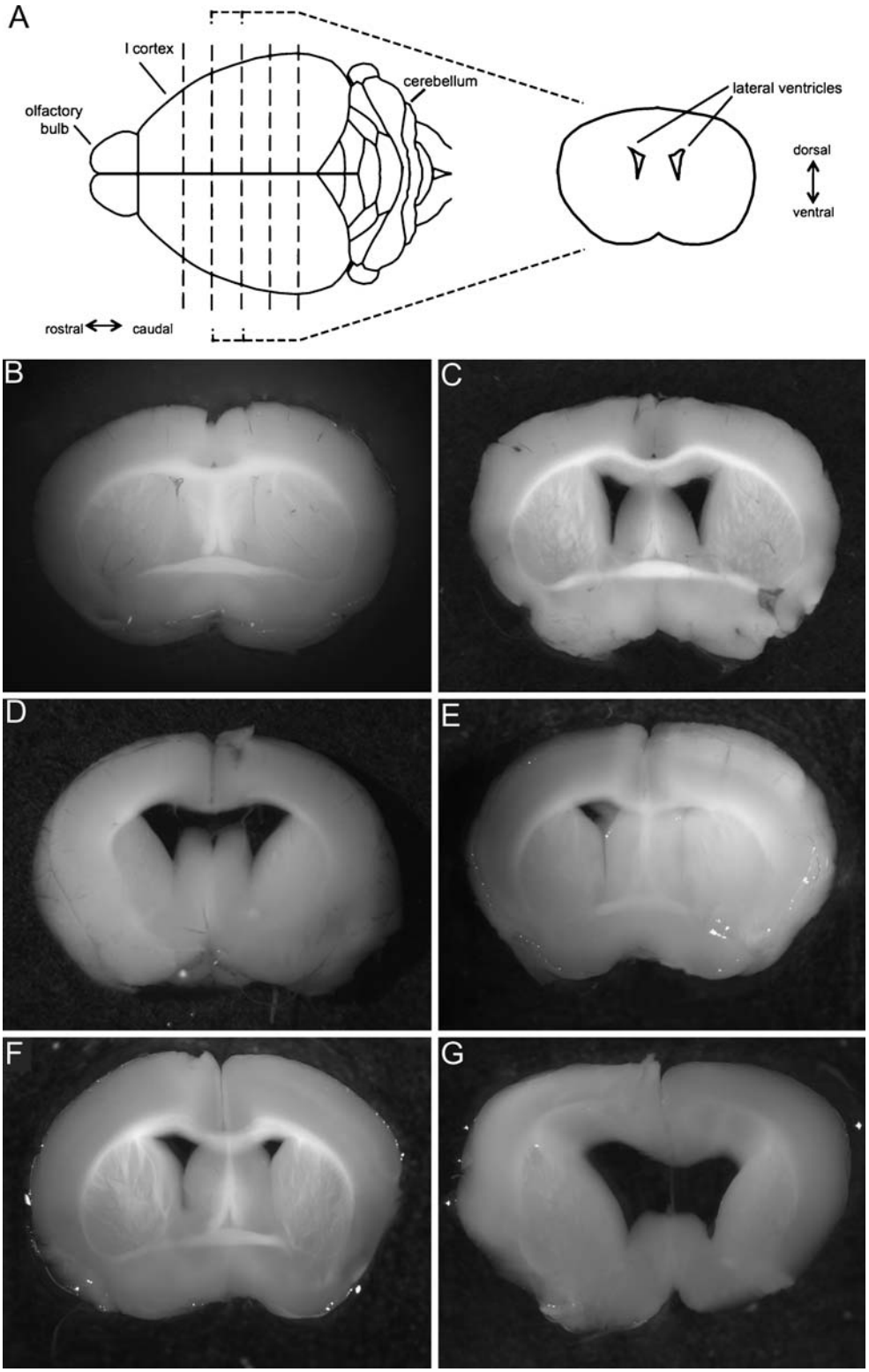

Fig. 1 The incidence and severity of hydrocephalus varies among *L1-6D* mutant mice. **a** Diagram of a mouse brain (dorsal view) and a traced coronal section. *Dotted lines* represent the approximate positions of coronal sections. ImageJ software was used to trace the perimeters and calculate the areas of the cerebral cortex section and both lateral ventricles. **b** A recently weaned 129.Cg-*L1cam-6D* mouse with ventricles of normal size. **c**, **d** Two different B6.Cg-*L1-6D* mutant mice with hydrocephalus: (**c**) adult and (**d**) weanling. **e**–**g** Three recently weaned F2 *L1-6D* mutant mice demonstrating the varying severity of hydrocephalus observed among affected mutants in the F2 generation

Mice were initially classified as hydrocephalic (affected) or non-hydrocephalic (unaffected) based on the appearance of the lateral ventricles. Mice were categorized as unaffected, if both of their lateral ventricles were shaped like thin slits. However, if at least one lateral ventricle was expanded, the mouse was categorized as hydrocephalic. Microscope-attached digital cameras (Nikon and RT Slider Diagnostic Instruments, Inc.) were used to image one or two sections showing the lateral ventricles.

The hydrocephalic phenotype of F2 *L1-6D* mice utilized for linkage analyses was quantified as follows. For each mouse, we chose the imaged section that showed the greatest expansion of the lateral ventricles. The positions of these sections corresponded to reference sections positioned within +1.0 mm from Bregma [61]. Next, the perimeter of the coronal section and its respective lateral ventricles were manually traced with ImageJ software [62]. ImageJ was then further utilized to calculate the areas of the traced regions. This generated three measurements: coronal section area, left ventricle area, and right ventricle area. Left and right ventricle areas were added together to calculate total lateral ventricular area. To account for differences in brain size and standardize measurements, a ratio was calculated for each brain: total lateral ventricular area divided by coronal section area. Ratios were then transformed, using a natural log scale [ln (1,000×ratio)], to approximate a normal distribution for statistical analyses. We refer to these transformed ratios as hydrocephalus severity scores. Student's *t* tests were performed to determine whether there were significant differences in hydrocephalus severity between the different cohorts, as well as between the two sexes.

Genotyping

Genomic DNA was obtained from mouse toes and/or tails. Tissue samples were digested overnight with Proteinase K. *L1-6D* genotyping was performed using PCR amplification and the following primer set: forward 5′- CCAGCCAGGATCC TAACAAAAGAC, reverse wild-type allele 5′- AGT GATGCTGGCCTGCAAAG, and reverse knock-in allele 5′- AACCACACTGCTCGACCTG. In preparation for single nucleotide polymorphism (SNP) genotyping, genomic DNA was treated with a RNAse A/RNAse T cocktail (Ambion) and purified using either Puregene Blood Core Kit B (Gentra Systems, Qiagen) or DNeasy Blood and Tissue Kit (Qiagen, Cat. no. 69504). DNA concentrations were measured with a Nanodrop ND-1000 Spectrophotometer.

The genome-wide scan was performed at the Affymetrix GeneChip laboratory of the Yale Microarray Center for Research on the Nervous System, through the NIH Neuroscience Microarray Consortium. Illumina's Mouse Low Density Linkage panel and Golden Gate Assay were used to genotype 92 F2 *L1-6D* homo-/hemizygote pups with hydrocephalus at 377 SNPs; 99% of the genotypes were present. Genotypes were classified as 129S2 or C57BL/6J, and SNP performance was evaluated by the Mouse SNP Genotyping Service at Harvard University. The genotypes of our 129S2 mice matched that of 129S1 mice at all 375 working SNPs except one (rs13481099), which appeared monomorphic between our 129S2 and C57BL/6J mice. Ultimately, 246 informative SNPs were polymorphic between 129S2 and C57BL/6J mice; the average genomic distance between these SNPs was 9.9 Mb.

We verified that all F2 *L1-6D* mice carried the *L1-6D* associated 129/Sv congenic interval by sequencing SNP rs3157210, located between exons 1 and 2 in the *L1cam* gene. The following primers were used to amplify a 495 base pair fragment containing rs3157210: forward 5′- CACTCCACAATAGCCACACAC and reverse 5′- GCCCTCACTTCTTCTGTAAC. PCR products were then treated with ExoSAP-IT (USB) to remove excess primers and nucleotides, and they were sequenced with Finnzymes' Phusion High Fidelity PCR Master Mix with HF buffer (New England Biolabs) and primer 5′- GCTGTTGAGTCAAGACCTGG.

Seven candidate modifier regions were selected for further analyses based on their linkage data. SNPs in these regions were chosen using the information obtained from the Mouse Phenome Database (http://phenome.jax.org). Genotyping was performed by the High Throughput Sequenom and Illumina Genotyping Facility at the Harvard Partners Center for Genetics and Genomics utilizing iPLEX Gold chemistry from Sequenom. Ultimately, 43 polymorphic SNPs, three to eight SNPs per candidate region, passed the performance criteria set by the Harvard Partners Center (Supplemental Table 3). These SNPs were employed to genotype the 92 F2 *L1-6D* mice with hydrocephalus originally utilized for the genome-wide scan, the additional F2 *L1-6D* mice used for the extension study (64 F2 *L1-6D* mice with hydrocephalus and 30 F2 *L1-6D* mice without hydrocephalus), and mice from the two parental strains (two B6.Cg-*L1-6D* mice and two 129S2.Cg-*L1-6D* mice).

Linkage analysis

Linkage analysis was performed using a total of 288 SNPs (272 autosomal and 16 X-linked). Mice with hydrocephalus and those without were analyzed separately. In addition, sex was used as a covariate. Data from male and female mice were analyzed separately, as well as combined and analyzed together. Progeny 6.9.04 software was used to visualize haplotypes.

To test for linkage to hydrocephalus susceptibility modifier loci, genotype frequencies at each marker were tested for departures from Mendelian segregation with chi-square goodness-of-fit tests, two degrees of freedom, using SAS software (SAS Institute, Inc., Version 9.1.3) [63, 64]. Fisher's exact tests were used to generate *p* values for each marker. However, when the frequency of a genotype at a marker is 0, an exact test cannot be performed. In those cases (see Supplemental Table 4), an asymptotic chi-square test was done.

Bonferroni adjustments (α=0.05 and α=0.005) were used to correct *p* values for multiple testing across SNPs: α

divided by the number of markers. During the original genome-wide scan, 229 autosomal markers were tested. Hence, we used Bonferroni thresholds of $\alpha/229$ to interpret the data. During the extension study, 43 additional autosomal SNPs were analyzed. To maintain stringent standards, extension study data were corrected utilizing all 272 autosomal markers (43 extension study markers + 229 autosomal markers): $\alpha/272$.

To interpret X-chromosome marker data, we had to analyze the two markers positioned inside the *L1-6D* 129 associated region (gnfX.035.350 and rs13483765) separately from the rest ($N=14$), which are positioned outside of the region. This distinction was necessary because F1 *L1-6D/L1-6D* homozygote females were 129 homozygotes within the region and F1 *L1-6D/+* females were 129/B6. When performing chi-square tests, we also separately analyzed male and female F2 progeny derived from the two F1 crosses: (1) *L1-6D/L1-6D* homozygote females bred to *L1-6D/Y* males and (2) *L1-6D/+* females bred to *L1-6D/Y* males. Depending on the type of F1 cross, the genotype frequencies expected for X-chromosome SNPs far away from *L1cam* (unlinked) vary. F2 *L1-6D* hemi-/homozygotes derived from F1 *L1-6D/L1-6D* females are expected to exhibit the following genotype frequencies: females—50% B6 homozygotes, 50% B6/129 and males—50% B6 hemizygotes, 50% 129 hemizygotes. On the other hand, 100% of the F2 *L1-6D/L1-6D* females derived from F1 *L1-6D/+* females are expected to be 129/B6, and 100% of the generated F2 *L1-6D/Y* males are expected to be 129 hemizygotes.

R/qtl 1.07-12 software was used for QTL analyses to test for linkage to severity modifier loci [65]. Single-locus and two-QTL, two-dimensional genome-wide scans, using a multiple imputation method with 2.5-Mb steps over the entire genome and 200 imputations, were performed utilizing 229 autosomal genome-wide markers. In addition, permutation tests were applied to single-locus and two-QTL scans as recommended for an intercross (http://www.rqtl.org/tutorials/). Multiple QTL mapping functions were also implemented (source: http://www.rqtl.org/multqtlfunc.R). Using recommended LOD thresholds [65], the results from the two-dimensional scan were summarized. The two-dimensional scan summary was then used to fit a multiple QTL model utilizing the "fitqtl" function in R/qtl.

As described in Broman et al. [66], R/qtl was also used to perform genome-wide scans that analyzed 14 X-chromosome markers along with all 229 autosomal markers. The X-chromosome markers gnfX.035.350 and rs13483765, which are positioned within the 129 congenic interval present in all *L1-6D* mutants, were excluded. Thirty-nine F2 *L1-6D* hemi-/homozygous mutants derived from F1 *L1-6D/L1-6D* females were used for the X-chromosome R/qtl study. F2 *L1-6D* mutants derived from F1 *L1-6D/+* females were excluded from the analysis because their siblings were not genotyped and the missing data would confound analysis.

In addition, R/qtl was used to analyze data from the extension study. Three sets of analyses were conducted. First, the cohort of 64 F2 *L1-6D* mutants with hydrocephalus (utilized solely for the extension study) was examined at the 43 extension study SNPs. Second, the complete group of 156 F2 *L1-6D* hydrocephalic mutant mice (64 + 92 from the original genome scan) was examined at the 43 extension study SNPs. Lastly, the original 92 F2 *L1-6D* mice with hydrocephalus utilized for the genome-wide scan were analyzed with the complete set of 272 autosomal markers (229 original SNPs + 43 new validation study SNPs). In addition, cohorts were divided by sex, and males and females were analyzed separately. Single-locus effect plots and two-loci interaction effect plots were generated with R/qtl.

As an alternative test for severity modifiers, F2 *L1-6D* hydrocephalic mutant mice were classified as having moderate or severe hydrocephalus based on whether their hydrocephalus severity score was higher or lower than the median hydrocephalus severity score of all F2 *L1-6D* hydrocephalic mutant mice. A chi-square test with two degrees of freedom was performed to compare genotype frequencies between the moderate and severe hydrocephalus groups.

Microarray analysis

Gene Expression Omnibus (GEO) data set GDS 1490 was downloaded from http://www.ncbi.nlm.nih.gov/geo. Normalized TeraGenomics-calculated signal intensities and detection calls were obtained for 91 Affymetrix Murine Genome U74AV2 gene chips comprising 24 neural tissues in C57BL/6J and 129S6/SvEvTac mice [67]. Replicates were pooled, and mean fold changes were calculated using Spotfire DecisionSite (TIBCO, Version 9.1.1). Statistical analyses were not performed to determine significant differences because of the small sample size. Each condition had only two replicates, except for the CA1 region of the hippocampus, which had three replicates.

In addition, our lab performed a microarray experiment: GEO data set GSE13984. RNA was purified from the cerebellums of three postnatal day11 congenic 129S2 *L1cam* knock outs (129S2.Cg-*L1cam*^{tm1Sor}) and three of their wild-type siblings utilizing Qiagen's RNeasy Mini kit (no. 74104). Therefore, each genotype, *L1KO* and wild type, had three replicates. Samples were processed at the Case Western Reserve University Cancer Center Gene Expression Array Core Facility and hybridized to Affymetrix Murine Genome U74AV2 gene chips. Affymetrix GeneChip Operating Software was used to process gene

chip images and generate MAS 5.0 signal intensities and detection calls. Replicates were normalized by the mean signal value of all probes and then pooled using Spotfire DecisionSite. Significance was determined by performing an unpaired two-tailed Student's *t* test on normalized signal intensities.

Results

Strain-specific modifiers contribute to hydrocephalus in *L1-6D* mice

The incidence of hydrocephalus differs among strains of *L1cam* mutant mice. Severe hydrocephalus is evident in C57BL/6J, but not 129/Sv, *L1cam* mutants. To identify modifier loci that interact with *L1cam* to cause X-linked hydrocephalus, we performed linkage analyses on *L1cam* mutants derived from the breeding of 129S2 and C57BL/6J mice. To generate sufficient mice for the study, we utilized *L1-6D* knock-in mice rather than *L1KOs*. Unlike *L1KOs*, which fail to express L1, *L1-6D* knock-in mice express a mutant protein in which the sixth Ig-like domain of L1 has been deleted [60]. This Ig-like domain, which contains two Arg-Gly-Asp (RGD) sequences, is required for L1 homophilic (L1-L1) and L1-integrin binding in vitro; yet, despite the deletion, the L1-6D protein retains some function. Its interactions with Neurocan and Neuropilin-1 are preserved, and in contrast to *L1KOs*, *L1-6D* mutants develop a normal corticospinal tract. Nevertheless, *L1-6D* mutants, like *L1KOs*, have been observed to exhibit hydrocephalus, on the C57BL/6J, but not 129S2 background [60].

Consistent with these findings, we found that the incidence of hydrocephalus differs between our congenic *L1-6D* C57BL/6J (B6.Cg-*L1-6D*) and 129S2 (129S2.Cg-*L1-6D*) mice. Coronal sections were prepared from *L1-6D* mutant (*L1-6D/Y* hemizygotes and *L1-6D/L1-6D* homozygotes) mice of varying ages, p21-adults (Fig. 1a). Dramatic hydrocephalus was evident in all B6.Cg-*L1-6D* mutant mice analyzed (N=10; Fig. 1c, d). However, hydrocephalus was seldom seen in 129S2.Cg-*L1-6D* mutant mice (Fig. 1b). Only two of 36 mice (5.6%) exhibited mild hydrocephalus (data not shown). Hence, our congenic *L1-6D* lines could validly be used to identify modifier loci that (1) are polymorphic between the two strains and (2) influence the manifestation of *L1cam* X-linked hydrocephalus.

In addition, the use of *L1-6D*, rather than *L1KO* mice, was advantageous because *L1KO* (*L1cam*^{tm1Sor}) males are infertile (Supplemental Text 1). On the other hand, 129S2.Cg-*L1-6D* hemizygous males (*L1-6D/Y*) are fertile, and their fertility permits the generation of *L1-6D* homozygous females, which are also fertile. The ability to breed *L1-6D* hemi- and homozygous mutants allowed us to generate sufficient mutants for linkage mapping, despite the significant pre- and postnatal mortality caused by *L1cam* mutations (Supplemental Text 2).

This early mortality phenotype, prevalent among both *L1-6D* 129S2 and C57BL/6J mice, contrasts with the severe hydrocephalus phenotype, which is strain specific. Hence, while modifier loci may influence both mortality and hydrocephalus in *L1cam* mutants, the data suggest that modifier loci that contribute to non-lethal severe hydrocephalus play a major role in the development of hydrocephalus. Since we evaluated all mice for hydrocephalus after weaning, our study was designed to identify this latter class of modifiers.

As illustrated in our breeding scheme (Fig. 2), we first mated B6.Cg-*L1-6D/+* females to 129S2.Cg-*L1-6D/Y* males. We evaluated 16 F1 *L1-6D* hemi-/homozygous mutants, between p21 and 3 months of age, for the phenotype. None exhibited hydrocephalus, demonstrating that primary (main-effect) hydrocephalus-causing modifiers do not act in a dominant manner. This observation additionally suggests that if a main-effect modifier is inherited from the C57BL/6J strain, it is not sex-linked. If it were, we would expect F1 *L1-6D/Y* males to exhibit hydrocephalus since their X chromosome, which carries the *L1-6D* mutation, was inherited from the C57BL/6J strain.

Next, we set up an intercross between F1 *L1-6D/Y* 129/B6 males and F1 *L1-6D* homo- or heterozygote 129/B6 females. We implemented this breeding scheme, which provided opportunities for meiotic recombination between the 129S2 and C57BL/6J chromosomes of both parents, to facilitate linkage analysis. Based on this cross (Fig. 2), if the C57BL/6J allele of one recessive, fully penetrant modifier gene caused hydrocephalus, one would expect 25% of F2 *L1-6D* mutants to be B6 homozygotes at the modifier locus and consequently exhibit hydrocephalus. We evaluated 1,058 F2 *L1-6D* mutants, between p21 and p39, for the phenotype. Strikingly, 31.9% of them exhibited hydrocephalus with variable severity (Fig. 1e–g): N=338 hydrocephalic F2 *L1-6D* mutants (199 *L1-6D/Y* males and 139 *L1-6D/L1-6D* females). In contrast, the phenotype was not observed in any F2 wild-type siblings (N=27). While 5.3% of F2 *L1-6D/+*

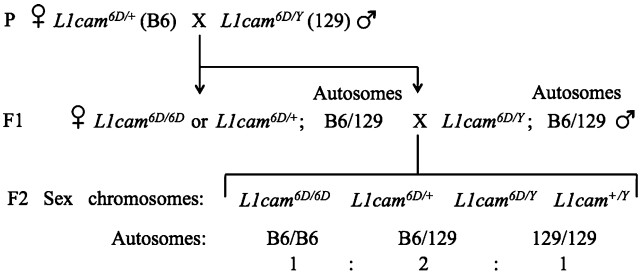

Fig. 2 Breeding scheme used to map modifier loci that contribute to *L1cam* X-linked hydrocephalus

heterozygote siblings (two of 38) exhibited hydrocephalus, the phenotype was much less severe than that exhibited by F2 *L1-6D* hemi-/homozygotes (data not shown).

Based on these data, we hypothesized that main-effect hydrocephalus susceptibility modifiers, which determine the presence or absence of the hydrocephalus phenotype in *L1cam* mutants, act in a recessive manner. In addition, since 129S2 *L1-6D* mutants seldom exhibit hydrocephalus, we expected C57BL/6J alleles at main-effect loci to be primarily responsible for causing the phenotype. Furthermore, since the severity of the phenotype varied among F2 mutants, we hypothesized that hydrocephalus is a complex trait, whose severity is affected by multiple, interacting loci.

Genome-wide scan identifies multiple candidate modifier loci

To identify the chromosomal location of *L1cam*-associated hydrocephalus modifier loci, we conducted a linkage study with an initial genome-wide scan on 92 F2 *L1-6D* mice with hydrocephalus. This group consisted of 55 *L1-6D/Y* males and 37 *L1-6D/L1-6D* females, whose ages ranged from postnatal day21 to 30. To quantify the phenotype, a representative coronal section was analyzed for each individual. The areas of both lateral ventricles and the brain section were measured. Total ventricular area was then divided by total brain area to normalize measurements, and values were transformed for statistical analyses. We refer to these transformed values as the hydrocephalus severity score. Figure 3a illustrates the distribution of hydrocephalus severity among the 92 F2 *L1-6D* mutants. Mice were also separated by sex to compare the distribution of hydrocephalus severity scores in males versus females (Fig. 3b–c). In this cohort of 92 mice, males tended to exhibit slightly more severe hydrocephalus than females, $p<0.05$.

Each mouse was genotyped at 245 informative SNPs, which were polymorphic between the C57BL/6J and 129S2 strains. Since our goal was to uncover both hydrocephalus susceptibility and severity modifiers, we utilized two distinct approaches for data analyses. Chi-square tests for Mendelian segregation were used to identify candidate susceptibility loci. Meanwhile, QTL analysis was employed to detect candidate severity loci.

We commenced our search for candidate susceptibility markers by testing each marker for linkage to the hydrocephalus phenotype. Based on the breeding scheme (Fig. 2), we hypothesized that autosomal markers *not* linked to hydrocephalus would exhibit the expected 1:2:1 Mendelian ratio of B6/B6:B6/129:129/129. In contrast, we expected the genotype frequencies of markers linked to hydrocephalus to deviate from Mendelian segregation. Since hydrocephalus was universally seen in congenic C57BL/6J *L1-6D* mutants, but only seldom seen in congenic 129S2 *L1-6D* mutants, we hypothesized that the frequency of B6 homozygotes at autosomal SNPs linked to hydrocephalus would significantly exceed 25%. A chi-square goodness-of-fit test was utilized to compare the observed genotype frequencies at each SNP (N=229 autosomal SNPs) with those expected based on Mendelian segregation.

Four genomic regions, located on chromosomes 2, 3, 4 and 5, exhibited deviations from Mendelian segregation, $p<0.001$ (Table 1). In these regions, a greater percentage of F2 *L1-6D* mutants were B6 homozygotes than expected. Rather than 25% of the mice being B6 homozygotes, more than 42% were B6 homozygotes. This is consistent with the hypothesis that B6 alleles at modifier loci near these SNPs contribute to hydrocephalus. Based on the stringent criteria proposed by Lander and Kruglyak for genome-wide significance using F2 intercross progeny (two degrees of freedom), these findings would be classified as evidence of suggestive linkage because $p < 1.6 \times 10^{-3}$ [68]. Moreover, multiple markers on chromosomes 2, 3 and 5 surpassed Lander and Kruglyak's significant linkage threshold of $p < 5.2 \times 10^{-5}$ and retained significance after a Bonferroni adjustment (α=0.005) was used to correct for multiple testing of the null hypothesis.

Chi-square tests for deviations from Mendelian segregation were also separately performed on males and females. The same regions on chromosomes 2, 3, and 5, which were specified above, exhibited deviations from Mendelian segregation in both sexes, $p<0.01$ (Supplemental Table 1). In contrast, linkage evidence for the region on chromosome 4 differed between the sexes. At one marker (rs3023025), females showed no evidence of linkage ($p>0.05$), while males exhibited suggestive linkage $\left(p = 9.25 \times 10^{-4}\right)$. However, this p value did not pass Bonferroni correction (α=0.05). Hence, our data do not provide evidence that loci on chromosome 2, 3, 4, or 5 contribute to the development of hydrocephalus in one sex but not the other.

We then performed QTL analysis to map candidate hydrocephalus severity loci. R/qtl software was used to analyze the data collected from the aforementioned 92 F2 *L1-6D* hydrocephalic mutants. Associations between marker genotypes at 229 genome-wide autosomal SNPs and hydrocephalus severity scores were investigated. QTL analysis showed no main-effect loci linked to hydrocephalus severity. We found a linkage peak on chromosome 10 at 119 Mb (mCV25429984) with a LOD score of 2.9 (Fig. 4). However, a permutation test of the single-locus scan did not indicate significant evidence of linkage at this locus. A two-loci scan was then performed. Three pairs of loci had overall LOD scores above 6 (full LOD) and interaction LOD scores, which measure the statistical interaction between loci, above 3.5: (1) chromosome 4 at 153.7 Mb and chromosome 9 at 112.2 Mb, (2) chromosome 5 at 109.2 Mb and chromosome 9 at 102.2 Mb, and (3)

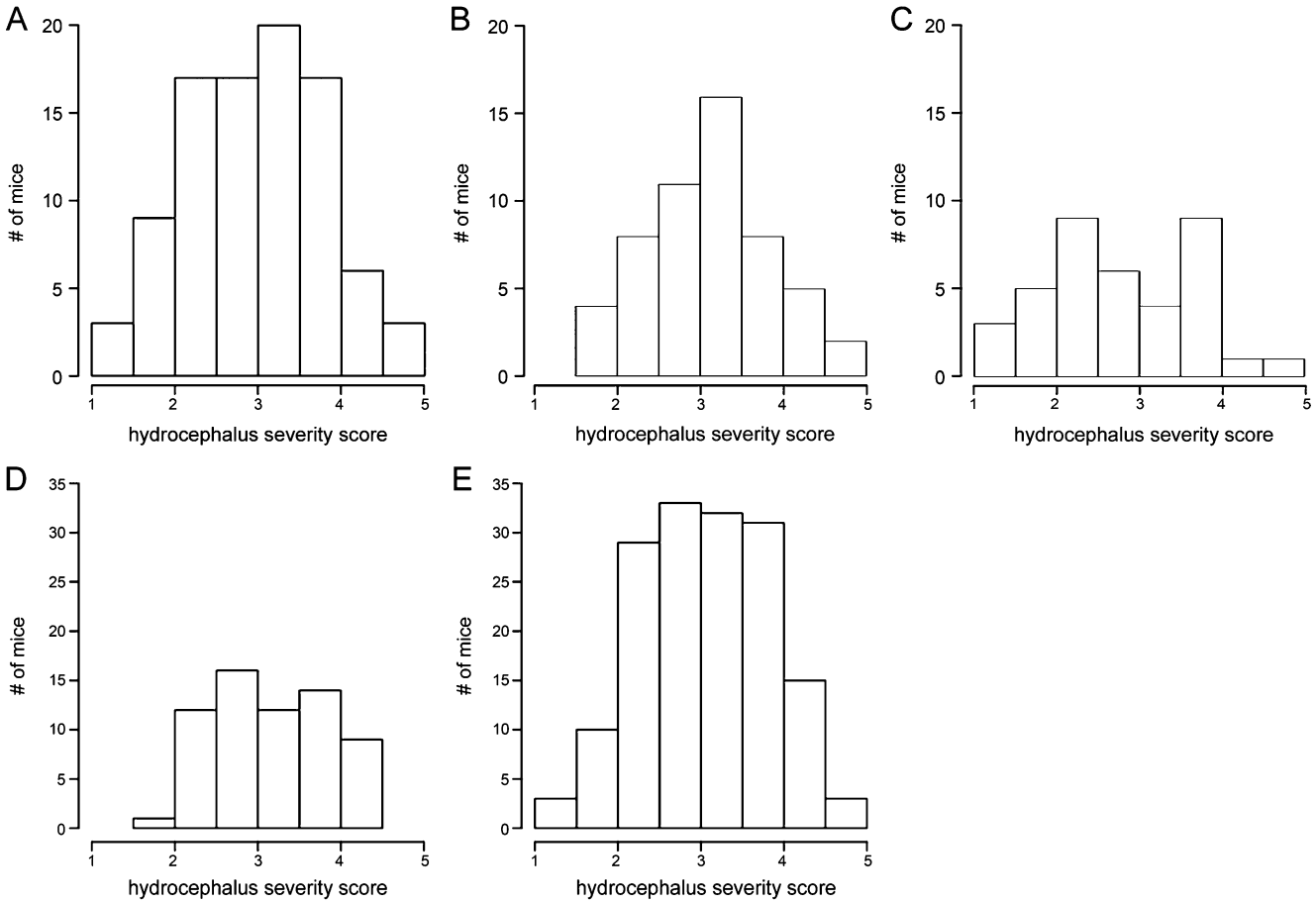

Fig. 3 Histograms illustrating the distribution of hydrocephalus severity among the different cohorts of F2 *L1-6D* mutant mice analyzed during the study. Hydrocephalus severity is plotted against the number of mice with scores in the specified range. Hydrocephalus severity increases along the *x*-axis. **a**–**c** Severity histograms for the 92 F2 *L1-6D* mutants analyzed in the genome-wide scan. **a** All mice. **b**, **c** Group segregated by sex: **b** males and **c** females. **d** Severity histogram for the 64 additional *F2 L1-6D* mutant mice used in the extension study. **e** Severity histogram representing the entire set (92+64) of 156 F2 *L1-6D* mutant mice with hydrocephalus

chromosome 7 at 101.6 Mb and chromosome 9 at 87.2 Mb (Supplemental Table 2). However, again, the permutation test revealed no significant results for this two-QTL scan. Furthermore, no QTLs were detected in males nor females when data were segregated by sex.

X-chromosome analyses

Analyses of the X chromosome required us to take into consideration that 129/Sv DNA was originally utilized to generate the *L1-6D* knock-in allele [60]. Consequently, all *L1-6D* C57BL/6J mice carry a 129 congenic interval, which includes the *L1cam* locus (positioned at 71.1 Mb). Sequencing revealed that this *L1-6D* associated 129 region is <25 Mb, and it lies between SNPs rs24884396 and rs3166693 (genome coordinates, 46.6–71.5 Mb).

Chi-square goodness-of-fit tests were performed on X-chromosome markers to test for departures from Mendelian segregation. Male and female progeny from the two F1 crosses, (1) *L1-6D/L1-6D* homozygote females bred to *L1-6D/Y* hemizygote males and (2) *L1-6D/+* females bred to *L1-6D/Y* hemizygote males, were analyzed separately. As expected, rs13483765, a SNP in the *L1-6D* associated 129 region positioned 16.3 Mb away from *L1cam*, showed linkage to hydrocephalus. Genotype frequencies at rs13483765 deviated from the Mendelian segregation expected of an unlinked marker (a marker far away from *L1cam*). A greater percentage of F2 *L1-6D/Y* males originating from F1 *L1-6D/L1-6D* females were 129 hemizygotes than expected for an unlinked X-chromosome marker; 129 hemizygosity was observed in 87% of the mice rather than in the expected 50%, $p = 4.88 \times 10^{-4} (N = 23)$. A valid analysis of rs13483765 in F2 *L1-6D/L1-6D* females derived from either cross, as well as in F2 males derived from F1 *L1-6D/+* females, was not possible. The sample sizes in these subgroups were too small.

A genome-wide QTL scan was also performed, including X-chromosome markers (14 X-chromosome markers + 229

Table 1 Candidate modifier loci identified through genome-wide chi-square tests for Mendelian segregation

SNP	Chr	Mb	Genotype			Exact *p* value
			B6/B6	B6/129	129/129	
rs4223428	2	120.322	39	43	10	1.07E−04[a]
rs8251635	2	125.128	41	41	10	1.98E−05[b]
rs3655895	2	144.359	41	40	11	3.10E−05[a]
rs13476832	2	149.561	42	40	10	8.53E−06[b]
rs6376291	2	153.967	42	40	10	8.53E−06[b]
rs13476892	2	165.222	42	36	14	2.60E−05[a]
rs3712766	2	165.836	42	34	15	2.31E−05[a]
rs3691114	3	59.630	43	31	17	9.06E−06[b]
rs6239288	3	60.315	44	31	17	4.50E−06[b]
rs3683507	3	79.005	45	30	17	1.36E−06[b]
rs13477223	3	80.666	45	29	18	1.13E−06[b]
rs3688780	3	86.177	42	32	18	3.52E−05[a]
rs4138858	3	87.446	41	33	18	9.73E−05[a]
rs3023025	4	142.772	39	39	14	3.97E−04
rs13478069	4	154.877	38	37	16	9.87E−04
rs3726547	5	108.813	41	38	13	5.36E−05[a]
rs3663141	5	117.205	41	41	10	8.53E−06[b]
rs3662161	5	117.909	42	40	10	1.98E−05[b]
gnf05.120.578	5	124.103	42	43	7	2.14E−06[b]

N=92 F2 *L1-6D* mice with hydrocephalus. The values reported in the Genotype columns denote the number of mice with the specified genotype

[a] Exact *p* value passed Bonferroni correction with α=0.05 and 229 SNPs

[b] Exact *p* value passed Bonferroni correction with α=0.005 and 229 SNPs

autosomal markers). The *L1-6D* associated 129 region was excluded because the 129/B6 genotype of parental females complicated the analysis. Furthermore, only 39 F2 *L1-6D* hemi-/homozygous mutants derived from F1 *L1-6D/L1-6D* females were used for the X-chromosome QTL study. F2 *L1-6D* mutants derived from F1 *L1-6D/+* females were not used because their siblings, non-hydrocephalic wild-type males and *L1-6D/+* females, were not genotyped with the genome-wide linkage panel. Since these F2 wild-type males and *L1-6D/+* females would have inherited their X chromosomes from the B6 parental strain, the missing data would confound analysis.

Single- and two-loci scans did not identify any X-chromosome markers linked to hydrocephalus severity. This result was not surprising, as the sample size was small. Furthermore, since the examined mice were all *L1-6D* hemi-/homozygotes with hydrocephalus of varying severity, there was no genetic variation at the locus to correlate with phenotype severity.

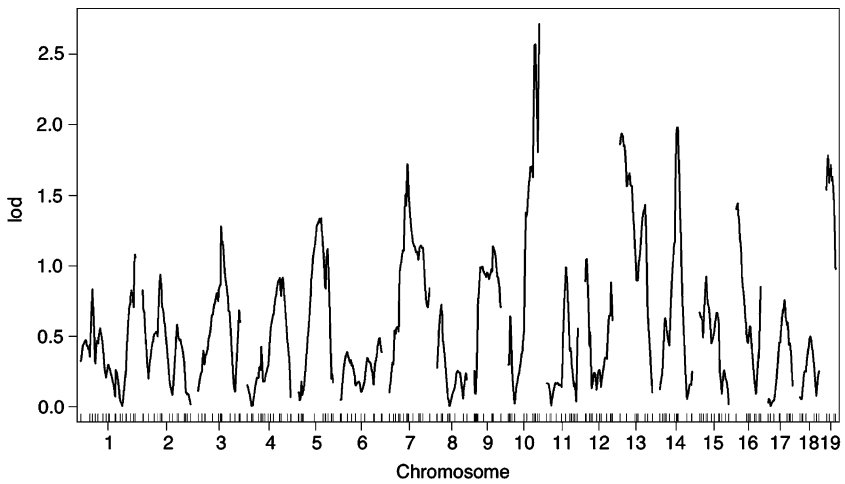

Fig. 4 LOD plot of a genome-wide scan for main-effect loci linked to hydrocephalus severity; 92 hydrocephalic F2 *L1-6D* mutants were genotyped at 229 informative autosomal markers

Extension study design

An extension study was next conducted to determine whether stronger linkage evidence could be obtained for the candidate modifier loci identified through the genome-wide scan. Seven genomic regions were analyzed in total. Two of these regions, located on chromosomes 4 and 5, were originally identified by both our chi-square analysis and two-loci QTL scan. Candidate modifier regions on chromosomes 2 and 3 were selected for further study based on their chi-square test results, while those on chromosomes 7 and 9 were chosen based on their two-loci QTL scan data. Lastly, a region on chromosome 10, surrounding rs3654717 (106.9 Mb), was further studied for two reasons. First, it was detected by the two-loci QTL scan, albeit with low LOD scores. When paired with a locus on chromosome 7 (60.2 Mb), the chromosome ten locus at 106.9 Mb had a full LOD score of 5.45 and an interacting LOD score of 0.261. Second, it was near the highest peak of the single-locus QTL scan.

For the extension study, 43 informative SNPs (Supplemental Table 3), dispersed throughout the candidate modifier regions, were used to genotype two new groups of mice: (1) a control set of 30 F2 *L1-6D* hemi/homozygous mutant siblings without hydrocephalus (unaffecteds) and (2) 64 additional F2 *L1-6D* hemi-/homozygous mutant mice with hydrocephalus (affecteds). Within this new cohort, the severity of hydrocephalus was not significantly different between males and females ($p>0.05$). Moreover, the severity of hydrocephalus exhibited by the new group of 64 F2 *L1-6D* mutants was not significantly different from that displayed by the original cohort of 92 F2 *L1-6D* mutants ($p>0.05$). Nevertheless, compared to the original cohort, a lower percentage of mice in the new group had hydrocephalus severity scores less than 2 (Fig. 3d). While 13% of the mice in the original cohort scored below 2, only 1.6% of the mice in the new cohort scored below 2. We preferentially chose mice with the most severe phenotype for the extension study because we thought that they might be enriched for individual alleles or combinations of alleles that have strong effects.

Identification of a *L1cam* hydrocephalus modifier locus on chromosome 5

The extension study replicated the results obtained for the candidate modifier region on chromosome 5. A chi-square test for deviation from Mendelian segregation was performed on the new cohort of 64 F2 *L1-6D* mice with hydrocephalus utilizing the chromosome 5 SNPs listed in Supplemental Table 3. All eight new markers exhibited deviations from Mendelian segregation; B6 homozygotes were more prevalent than other genotypes (Table 2). Six adjacent markers (100.1–120 Mb) demonstrated evidence for significant linkage, surpassing the $p < 5.2 \times 10^{-5}$ threshold proposed by Lander and Kruglyak [68]. Moreover, five of these markers retained significance following Bonferroni correction ($\alpha=0.005$).

The group was also divided by sex, and the region was separately tested for linkage among males and females. Original genome-wide scan results were replicated. Markers in the chromosome 5 candidate modifier region deviated from Mendelian segregation in both sexes, $p<0.005$ (Supplemental Table 4).

Moreover, combined analysis of all 156 F2 *L1-6D* mutants with hydrocephalus (64 from the extension study

Table 2 Extension study chi-square tests for Mendelian segregation on chromosome 5

Marker	Position (Mb)	64 new F2 *L1-6D* mutants with hydrocephalus				All 156 F2 *L1-6D* mutants with hydrocephalus				30 F2 *L1-6D* mutants without hydrocephalus			
		Genotype			Exact	Genotype			Exact	Genotype			Exact *p* value
		B6	H	129	*p* value	B6	H	129	*p* value	B6	H	129	
rs3688859	100.055	31	29	3	6.12E−06[a]	70	72	13	2.01E−09[a]	6	17	7	0.791
rs3694887	104.164	34	27	3	2.92E−07[a]	75	68	13	4.04E−11[a]	7	16	7	0.943
rs3654076	106.519	33	27	3	6.64E−07[a]	73	69	13	1.41E−10[a]	7	16	7	0.943
rs3665124	110.024	32	29	3	3.17E−06[a]	73	67	16	6.64E−10[a]	5	18	7	0.492
rs3657810	113.832	31	30	3	6.18E−06[a]	72	71	13	4.23E−10[a]	5	19	6	0.407
rs3653889	119.958	30	29	4	2.58E−05[b]	69	72	13	3.30E−09[a]	6	19	5	0.407
rs3710934	121.681	29	30	5	1.29E−04[b]	70	73	13	1.97E−09[a]	6	18	6	0.591
rs6345336	129.158	24	34	5	0.0025	65	77	13	5.06E−08[a]	6	18	6	0.591

Genotype: B6 = B6/B6, H = B6/129, 129=129/129

[a] Exact *p* value passed Bonferroni correction with $\alpha=0.005$ and 272 SNPs

[b] Exact *p* value passed Bonferroni correction with $\alpha=0.05$ and 272 SNPs

Table 3 LOD scores for interacting loci pairs

Interacting pair	Full LOD score	Interaction LOD score
Chr5 at 106.7 Mb : Chr9 at 102.2 Mb	7.23	4.58
Chr7 at 101.6 Mb : Chr9at 89.7 Mb	6.62	3.70

Data from genome-wide two-loci QTL scan performed on 92 hydrocephalic F2 *L1-6D* mice using 272 autosomal markers

and 92 from the original genome-wide scan) resulted in the significant linkage of the eight extension study SNPs. All markers passed Bonferroni correction (α=0.005), and the lowest p value was exhibited by rs3694887 (104.2 Mb), $p = 4.04 \times 10^{-11}$. Significant linkage was also observed in both sexes (Supplemental Table 4). Taken together, the genome-wide scan and extension study results confirm linkage of this region to hydrocephalus. We denote our newly discovered modifier locus on chromosome 5, which genetically interacts with *L1cam* to contribute to hydrocephalus as *L1cam hydrocephalus modifier 1* (*L1hydro1*). Based on our chi-square results and haplotype visualization, we propose that *L1hydro1* is located in the region between genome coordinates 100–129.2 Mb.

Interestingly, no single genotype in the *L1hydro1* region was shared between all hydrocephalic mice. This suggests that the *L1hydro1* modifier does not, on its own, account for all hydrocephalus cases. In addition, the genotype frequencies of F2 *L1-6D* mutant mice without hydrocephalus did not deviate from Mendelian segregation at *L1hydro1* (Table 2). If harboring a B6 homozygote genotype at *L1hydro1* causes hydrocephalus in *L1cam* mutants, few, if any, unaffected *L1-6D* mutants should be B6 homozygotes at *L1hydro1*. Rather, one would expect more hetero- or 129 homozygotes at *L1hydro1* in unaffected *L1-6D* mice, yet this was not seen. Taken together, these last two observations suggest that *L1hydro1* exhibits incomplete penetrance, i.e., some individuals carrying the allele that contributes to hydrocephalus fail to exhibit the trait.

Extension study analyses of candidate modifiers on chromosomes 2, 3, and 4

The extension study, performed on 64 new F2 *L1-6D* mutants with hydrocephalus, failed to detect linkage to markers on chromosomes 2 and 3. In contrast to data from the original genome-wide study, genotypes with significant deviations from Mendelian segregation were not observed (p>0.05). Furthermore, although four markers within a region on chromosome 4 (134.7–149.8 Mb) exhibited p<0.05, significance was not retained after Bonferroni correction (α=0.05). Hence, the extension study also did not validate linkage of the chromosome 4 locus.

Nevertheless, when we analyzed genotype frequencies for deviations from Mendelian segregation at the extension study SNPs utilizing our entire set of 156 F2 *L1-6D* hydrocephalic mutants, multiple markers on chromosomes 2, 3, and 4 surpassed Lander and Kruglyak's proposed $p < 1.6 \times 10^{-3}$ threshold for suggestive linkage. Furthermore, they retained significance after Bonferroni adjustment (α=0.05). One marker on chromosome 2 (rs13476825) and two markers on chromosome 4 (rs6191908 and rs3675987) even exhibited evidence for significant linkage, $p < 5.2 \times 10^{-5}$ (Supplemental Table 5).

Thus, while the extension study did not replicate results, the loci on chromosomes 2, 3, and 4 continued to exhibit evidence of linkage when the extension study set of mice were analyzed together with the original set of 92 mice. Hence, the regions remain candidate modifier loci. Indeed, while the loci may be false positives, it is also possible that these loci have smaller effects than the *L1Hydro1* locus and that our extension study lacked sufficient power to detect linkage. Alternatively, it may be that the loci contribute to milder forms of hydrocephalus and that the distribution of hydrocephalus severity within the extension study group prohibited detection.

QTL analyses of extension study data

Extension study data were also analyzed to determine whether candidate modifier loci affect hydrocephalus severity. QTL analyses were performed, using the 43 new extension study SNPs, on two groups: (1) the extension study cohort of 64 hydrocephalic F2 *L1-6D* mutant mice and (2) the entire set of 156 F2 *L1-6D* hydrocephalic mice. No linkage evidence was found. Individual loci did not show linkage, nor did any pair of interacting loci meet the recommended thresholds [65] for inclusion into a two-QTL model. While it is possible that the interacting loci on chromosomes 4, 5, 7, and 9, which were detected by the original two-loci QTL genome-wide scan, were false positives, the distribution of hydrocephalus severity in the new cohort may have prevented replication. In addition, our extension study may have been underpowered to identify multiple QTL that contribute to hydrocephalus severity but do not exhibit a strong individual effect.

We then reanalyzed our original 92 F2 *L1-6D* hydrocephalic mice with our entire set of 272 autosomal markers (246 original genome scan markers + 43 new extension study markers). Genome-wide single- and two-loci scans were conducted. Individual loci did not demonstrate linkage. In addition, this analysis revealed no evidence for a two-QTL interaction involving the chromosome 4 locus. Furthermore, while the three regions on chromosomes 5

(106.7 Mb), 7 (99.1 Mb), and 9 (92.2–102.2 Mb) again met thresholds for inclusion into a two-QTL model (Table 3), a permutation test indicated that the loci pairs still did not exhibit significant evidence of linkage.

We then examined the simultaneous effects of multiple QTLs by incorporating the four loci on chromosomes 5, 7, and 9 into a multiple QTL model. Individual loci, as well as pair-wise gene interactions, exhibited p values less than 0.005 (Table 4). Moreover, the full QTL model could explain 48% of the phenotypic variance associated with hydrocephalus $\left(p < 5.3 \times 10^{-6}\right)$. Hence, we continued to consider these three regions on chromosomes 5, 7, and 9 as candidate severity QTL.

To better understand the relationship between genotypes at these candidate QTL and hydrocephalus severity, we generated single-locus effect plots, comparing genotype to hydrocephalus severity (Fig. 5a–c). Mice with a B6/B6 genotype at marker rs3654076, located within the *L1hydro1* region on chromosome 5, tended to have more severe hydrocephalus than mice with the 129/B6 or 129/129 genotype (Fig. 5a). In contrast, mice with a 129/129 genotype at rs13479392, the marker linked to the candidate chromosome 7 QTL, tended to exhibit more severe hydrocephalus than mice with other genotypes at that marker (Fig. 5b). Single-locus effect plots for the two chromosome 9 markers, rs4138352 and rs3657346 (92.2–102.2 Mb), did not reveal substantial differences in hydrocephalus severity between different genotypes (Fig. 5c). However, interaction effect plots, which depict how genotypes at two-loci influence the phenotype, indicate that the severity of hydrocephalus exhibited by mice carrying a B6/B6 genotype at both chromosome 9 markers is augmented by B6 homozygosity at chromosome 5 (rs3654076) or 129 homozygosity at chromosome 7 (rs13479392; Fig. 5d–e). Taken together, all these effect plots suggest that C57BL/6J mice carry an allele on chromosome 5, within *L1hydro1*, that exacerbates the hydrocephalus phenotype. Furthermore, genotypes at *L1hydro1* may interact with genotypes at the candidate chromosome 9 QTL to affect severity. In turn, genotypes at the candidate chromosome 9 QTL may additionally interact with those at the third candidate severity QTL on chromosome 7.

A candidate hydrocephalus severity modifier on chromosome 10

As an additional approach to identify hydrocephalus severity modifiers, we conducted chi-square tests, comparing groups stratified by severity. Affected (hydrocephalic) mice were divided into two groups based on severity. First, all 156 hydrocephalic F2 *L1-6D* mutant mice were used to calculate the median hydrocephalus severity score, median = 3.04. Those with a hydrocephalus severity score lower than the median were classified as having moderate hydrocephalus, while those with a hydrocephalus severity score higher than the median were classified as exhibiting severe hydrocephalus. The null hypothesis was that Mendelian segregation would be observed in both the moderate and severe hydrocephalus groups. Next, all 156 mice were analyzed at the 43 new markers (Supplemental Table 3). Interestingly, a locus on chromosome 10 deviated from Mendelian segregation in the moderate ($p<0.05$), but not severe hydrocephalus group ($p<0.09$). A chi-square test, comparing the genotype frequency (B6/B6:B6/129:129/129) between the moderate and severe hydrocephalus groups, revealed a significant difference, $p<0.005$. More mice with moderate hydrocephalus were 129, rather than B6, homozygotes within the chromosome 10 candidate modifier region, and vice versa, more mice with severe hydrocephalus were B6, rather than 129 homozygotes (Table 5). These data suggest that a candidate severity modifier locus is located on chromosome 10 (104.4–108.2 Mb) and that moderate hydrocephalus correlates with 129 homozygosity at the locus.

Curiously, when mice were segregated into four groups according to sex and hydrocephalus severity (males or

Table 4 Multiple QTL model for hydrocephalus severity

Chromosomal location (Mb)	Nearest marker	Variance (%)	F value	p value
Chr5 at 106.7	rs3654076	17.88	2.33	0.00083
Chr7 at 99.1	rs13479392	15.58	3.76	0.00244
Chr9 at 92.2	rs4138352	16.06	3.89	0.00194
Chr9 at 102.2	rs3657346	17.30	4.19	0.00109
Chr5 at 106.7:Chr9 at 102.2		14.97	5.44	0.00067
Chr7 at 99.1:Chr9 at 92.2		13.53	4.92	0.00142
% variance explained by full model		48.0		5.3×10^{-6}

N=92 F2 *L1-6D* mutants with hydrocephalus. Variance indicates the percentage of phenotypic variance explained by the specified locus, interacting loci, or full model (including interaction effects). F values were generated by R/qtl through ANOVA analysis. p values reflect the effects that removal of the specified locus or interacting loci have on the model

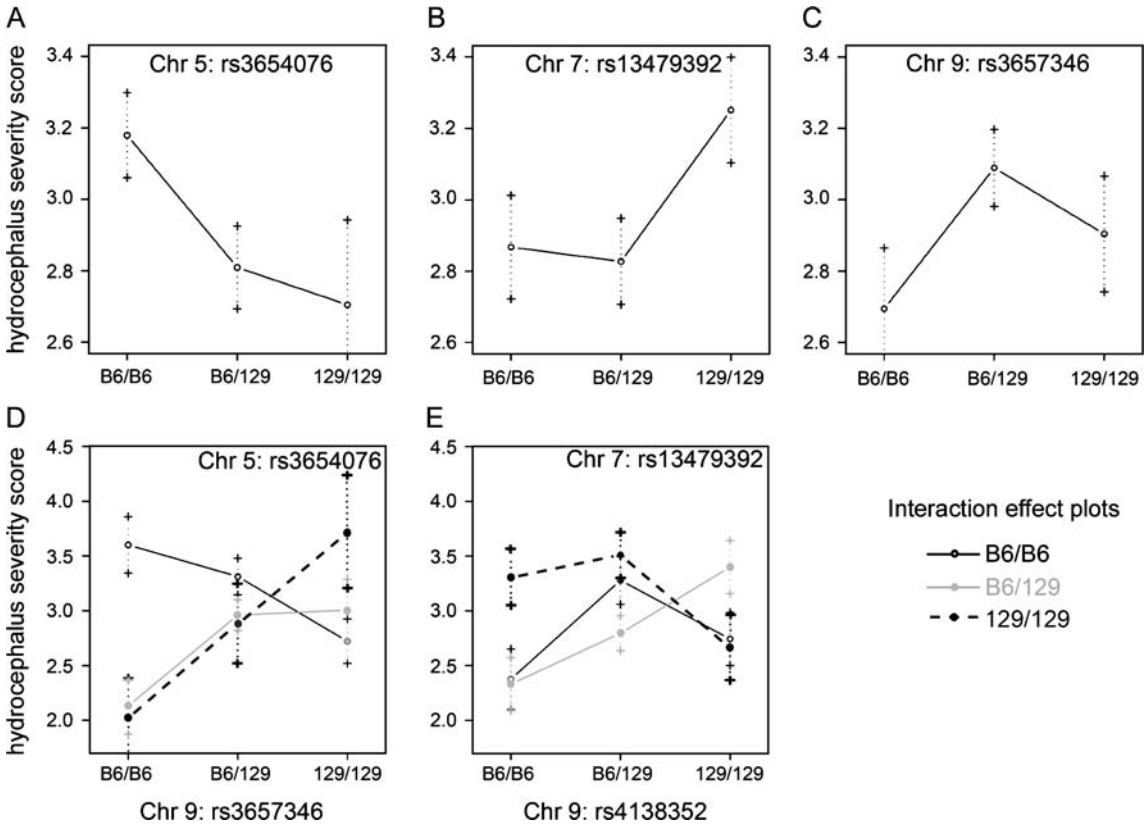

Fig. 5 **a**–**e** Effect plots depicting the effects of genotype on hydrocephalus severity at candidate QTL. Hydrocephalus severity increases along the *y*-axis. **a**–**c** Single-locus effect plots. Genotypes for the SNP listed at the top of each graph are indicated along the *x*-axis. The plot for the chromosome 9 SNP rs4138352 is similar to the one for rs3657346 (data not shown). **d**, **e** Interaction effect plots depict how the combinations of genotypes at two-loci influence severity. Genotypes for the SNP at the bottom of each graph are indicated along the *x*-axis. Genotypes for the second, interacting SNP (listed at the top of the graph) are *coded* according to the legend. *Error bars* represent ±SEM

females with moderate or severe hydrocephalus), only females with moderate hydrocephalus had genotypes that deviated from Mendelian segregation at the candidate chromosome 10 modifier locus, $p<0.05$ (Table 5). In this group, the incidence of 129 homozygotes was greater than expected. In contrast, we found no evidence that genotypes on chromosome 10 affect the phenotype of females with severe hydrocephalus or males. Nevertheless, the data do suggest that hydrocephalus severity differs between the sexes. A Student's *t* test, utilizing the entire set of 156 hydrocephalic F2 *L1-6D* mutants, indicated that females exhibit a slightly milder phenotype than males ($p<0.007$).

Table 5 Chi-square tests for Mendelian segregation in F2 *L1-6D* mice with moderate versus severe hydrocephalus

Group	Phenotype	Genotype at rs13480752			Exact *p* value	*p* value: genotype frequency comparison
		B6/B6 (%)	129/B6 (%)	129/129 (%)		
All mice	Moderate	14.3	50.7	35	0.034	0.003
	Severe	29.1	57	13.9	0.075	
Females	Moderate	8.1	51.4	40.5	0.021	0.006
	Severe	34.6	53.9	11.5	0.236	
Males	Moderate	20.5	48.7	30.8	0.689	0.196
	Severe	26.4	58.5	15.1	0.248	

$N=156$ affected F2 *L1-6D* mice. Percentages represent mice carrying the designated genotype in each hydrocephalus severity category. The exact *p* value was generated from a Fisher's exact test for deviation from Mendelian segregation within each phenotypic class. The second *p* value was obtained by comparing the moderate versus severe hydrocephalus genotype frequencies within each group. Neighboring SNPs rs6196597 and rs6243755 also had similar genotype frequencies (data not shown)

Our data raise the possibility that genotypes at the candidate chromosome 10 modifier may contribute to the observed sex difference by contributing to moderate hydrocephalus in females. However, the lack of correlation between 129 homozygosity at chromosome 10 and the phenotype of severely affected females indicates that if the locus is involved, it likely has a weak effect.

Expression analysis of genes in the *L1hydro1* region

The *L1hydro1* region, positioned between 100 and 129.2 Mb on chromosome 5, contains ~565 known and/or predicted Entrez listed genes (http://www.ncbi.nlm.nih.gov/sites/entrez). While finer mapping will be required to identify the gene(s) responsible for contributing to *L1cam* X-linked hydrocephalus, we surveyed the expression profiles of genes in the modifier region to gain insight about possible candidates. We utilized two sets of microarray data. One was a publicly available GEO data set, GDS1490, which included expression data from 24 neural tissues in C57BL/6J and 129S6/SvEvTac (129S6) mice [67], a substrain that like our 129S2 mice was derived from the 129S1 129/Sv strain [69]. The second data set, obtained in our lab, but previously unpublished, was an expression profile of cerebellar tissue from postnatal day 11 congenic 129S2 *L1cam* knock-out mice and their wild-type siblings (GEO data set: GSE13984).

Forty-three genes within the *L1hydro1* region were differentially expressed in neural tissues between C57BL/6J and 129S6 mice by ≥1.5 fold (Supplemental Table 6). *RIKEN cDNA 2310001H12*, a predicted gene containing a Krüppel-associated (KRAB) box and a zinc finger domain, demonstrated the greatest difference in expression. It was upregulated 4.4-fold in the choroid plexus of 129S6 mice compared to C57BL/6J mice. The choroid plexus is the highly vascularized ependymal structure that lines the ventricles of the brain and produces cerebrospinal fluid (reviewed in [70]). *Metal response transcription factor 2* (*Mtf2*) exhibited the second greatest difference in expression. It was 3.81-fold higher in the choroid plexus of 129S6 versus C57BL/6J mice. *Mtf2* encodes a polycomb-like protein. Polycomb group proteins silence transcription by binding and methylating nucleosomes (reviewed in [71]). Interestingly, *Mtf2* mutant mice exhibit hydrocephalus [8].

A few other genes that might play roles in *L1cam* function and/or hydrocephalus were also differentially expressed. For example, the genes encoding integrin binding *secreted phosphoprotein 1* (*Spp1*/*osteopontin*) ([72], reviewed in [73]) and extracellular matrix-associated protein *Sparc-like 1* (*Sparcl1*) [74] were upregulated in the choroid plexus of 129S6 versus C57BL/6J mice: 2.05- and 2.04-fold, respectively. Both *Sparcl1* and *Spp1*, like *L1cam*, regulate cell adhesion. In addition, *polycystin 2* (*Pkd2*) was expressed 1.5-fold higher in the choroid plexus of 129S6 than C57BL/6J mice. Pkd2, a member of the transient receptor potential (TRP) channel family, can function as an intracellular calcium release channel and as a cilium-anchored mechanosensory channel. In zebrafish, disruption of Pkd2 expression caused hydrocephalus [21]. Aside from differential expression in the choroid plexus, several genes in the *L1hydro1* region were also differentially expressed in other neural tissues.

Analysis of the microarray study conducted by our lab also provided some intriguing data. A total of three genes located within the *L1hydro1* region were differentially expressed in cerebellum between 129S2 congenic *L1KO* (129S2.Cg-*L1cam*^{tm1Sor}) and wild-type mice by at least 1.3-fold: *Mtf2*, *Pkd2*, and *cell division cycle 7* (*Cdc7*), which encodes a kinase involved in DNA replication [75]. All three genes were upregulated in wild-type mice, 1.79-, 1.36-, and 1.30-fold, respectively, compared to *L1KOs*. An unpaired two-tailed Student's *t* test was used to determine significance. While the *p* values generated by *Mtf2* and *Cdc7* ($p<0.02$) were significant, the *p* value for *Pkd2* was not ($p=0.17$). These results suggest a genetic interaction between *L1cam* and genes located within the *L1hydro1* region. Specifically, loss of *L1cam* seems to reduce the expression of *Mtf2* and *Cdc7*.

Discussion

A modifier locus on chromosome 5 contributes to *L1cam* X-linked hydrocephalus

We propose that manifestation of *L1cam* X-linked hydrocephalus in mice is affected by the functional status of the *L1cam* gene, as well as by the genotype of a modifier locus on chromosome 5. As previously discussed, X-linked hydrocephalus is evident in mice lacking all *L1cam* function (*L1KOs*), as well as in *L1-6D* mice, which have compromised L1-L1 homophilic and L1-integrin interactions. However, these mutations in the *L1cam* gene are not sufficient for the development of severe hydrocephalus. The phenotype is strain dependent. *L1KO* and *L1-6D* mutant mice develop severe hydrocephalus when bred on a C57BL/6J background. In contrast, 129S2 *L1KO* and *L1-6D* mutant mice do not. These data suggest that a locus, which is polymorphic between the two strains, interacts genetically with the *L1cam* gene to contribute to severe hydrocephalus.

Our work advances the current understanding of how hydrocephalus is caused by *L1cam* deficiencies by identifying a region on chromosome 5 (100–129.2 Mb) that behaves as a *L1cam* hydrocephalus modifier locus in mice. This locus, referred to as *L1hydro1*, surpassed Bonferroni

correction (α=0.005) and Lander and Krugylak's significant linkage threshold in both the original genome-wide scan and the extension study when analyzed with chi-square tests for deviations from Mendelian segregation. Furthermore, our multiple QTL model, which was generated through a different set of statistical analyses, suggests that the locus harbors a candidate severity modifier. Hence, *L1Hydro1* may affect both the severity of hydrocephalus in *L1cam* mutants and the susceptibility of *L1cam* mutants to the trait. As expected of a susceptibility modifier, a significantly greater number of hydrocephalic F2 *L1-6D* mutant mice were B6 homozygotes at *L1Hydro1* than predicted by Mendelian segregation. However, unaffected B6 homozygotes were also observed, suggesting that the modifier exhibits incomplete penetrance, a phenomenon often observed when a trait is influenced by the interactions of multiple loci.

Candidate regions for additional modifier loci

During the course of our analyses, we identified several candidate modifier loci with weak linkage evidence. These loci were found on chromosomes 2 (147.8–173.4 Mb), 3 (59.1–76.7 Mb), 4 (130.9–150.8), 7 (99.1 Mb), 9 (92.2–102.2 Mb), and 10 (104.4–108.2 Mb). While these loci may be false positives, it is also possible that some of these loci are modifiers with small effects on *L1cam* X-linked hydrocephalus. Our data may therefore help guide future studies.

Since the loci on chromosomes 2 and 3 were detected by chi-square tests for Mendelian segregation, they may affect how susceptible *L1cam* mutants are to hydrocephalus. On the other hand, the loci on chromosomes 7, 9, and 10 were identified as candidate severity modifiers. QTL analysis implicated the regions on chromosomes 7 and 9, while chi-square tests on groups segregated according to hydrocephalus severity detected the locus on chromosome 10. It is not surprising that these distinct approaches identified different candidate severity loci. While the stratified chi-square test dichotomizes the hydrocephalus phenotype (moderate versus severe), QTL analysis works with the full trait distribution. Furthermore, while QTL analysis considers gene–gene interactions, the stratified chi-square test can only evaluate only how individual loci affect severity.

Interestingly, the locus on chromosome 4 was detected by chi-square tests for Mendelian segregation, and it was implicated by QTL analysis. It is possible that this locus, like *L1Hydro1*, affects both susceptibility and severity.

Our findings suggest that X-linked hydrocephalus is a complex trait. Genotypes at *L1cam* and *L1hydro1* do not completely explain all hydrocephalus cases in the F2 generation. Hence, it is likely that *L1cam*-associated X-linked hydrocephalus is influenced by multiple genes. In addition, since the *L1-6D* mutation perturbs L1 homophilic and L1-integrin interactions [60], we suspect that disruption of these types of interactions plays an important role in the development of hydrocephalus.

Candidate modifier genes within the *L1hydro1* region

Taken together, our linkage data, microarray analyses, and published literature implicate *Mtf2*, as well as a few other genes, including *Pkd2*, as strong candidates for the modifier gene within *L1hydro1*. Strikingly, *Mtf2* (108.5 Mb) and *Pkd2* (104.9 Mb) even flank the chromosome 5 candidate severity QTL (106.7 Mb). In addition, *Mtf2* microarray results illustrate how the expression of the modifier gene in *L1hydro1* may be affected by genetic background. Data suggest that C57BL/6J mice express less *Mtf2* than 129S2 mice. Furthermore, *L1cam* knock-out mice exhibited decreased *Mtf2* expression compared to wild-type mice. Following this example, hydrocephalus may be prevalent in C57BL/6J but not 129/Sv *L1cam* mutants for the following reason: (1) *L1cam* mutants may express the modifier gene at lower levels than wild-type mice, and (2) C57BL/6J mice may exhibit decreased modifier gene expression compared to 129S2 mice.

Nevertheless, we also performed a more traditional search, utilizing NCBI databases such as PubMed and Entrez Gene, to search for additional candidate modifier genes within the *L1hydro1* region. *Fibroblast growth factor receptor like-1* (*Fgfrl1*) emerged as an intriguing candidate because L1 has been shown to directly bind FGFR [38]. *Mapk10* (*JNK3*) is also an interesting candidate because pharmacological studies suggest that inhibition of the JNK pathway affects L1 function (unpublished results). Furthermore, we consider *transforming growth factor beta receptor III* (*Tgfβr3*) a strong candidate because the receptor binds TGFβ1 [76], as well as other TGFβ superfamily members [77]. Transgenic mice that overproduce active *Tgfβ1* in the CNS develop hydrocephalus [14]. Lastly, two dynein subunits in the region, *Dynein light chain LC8-type 1* (*Dynll1*) and *Dynein axonemal heavy chain 10* (*Dnahc10*) stood out because loss of function of a related gene, *Dynein axonemal heavy chain 5* (*Dnahc5*), results in hydrocephalus [20].

Future work will aim to narrow down the *L1hydro1* region and identify the modifier gene. The creation of *L1-6D* 129S2 congenic mice that are B6 homozygotes within the *L1hydro1* interval should facilitate mapping and gene identification, as mice that carry the B6 allele at the modifier locus are expected to exhibit hydrocephalus. On the other hand, sequencing candidates may not be very informative. For example, sequence information from the Mouse Phenome Database indicates that several of the candidate genes discussed above contain nonsynonymous SNPs in their coding regions, yet, whether these polymorphisms contribute to hydrocephalus cannot be known without more functional experiments.

Human homologs in the *L1hydro1* region

The genes within the *L1hydro1* region have 297 human homologs (www.ensembl.org). Syntenic tracts of the *L1hydro1* region are dispersed throughout several human chromosomes. Most of the *L1hydro1* region maps to human chromosomes 1, 4, 12, and 22. However, there are also a small percentage of genes on the human X chromosome as well as on chromosomes 5, 11, and 16. Our search through the Pubmed and OMIM databases revealed no genes homologous to those in the *L1hydro1* region that have previously been associated with human hydrocephalus.

In conclusion, the identification of the *L1hydro1* locus and additional candidate modifier loci has driven the field closer to characterizing genes that contribute to hydrocephalus and genetically interact with *L1cam*. The insights obtained from this line of study will help determine whether genes that influence the development of congenital hydrocephalus in the mouse have similar roles in humans. The discovery of *L1cam* modifier genes will enhance our understanding of the molecular and cellular pathology of congenital hydrocephalus, a complex trait that develops from the interplay of multiple genetic factors. Furthermore, by elucidating the relationships between *L1cam* and its modifier genes, we will better comprehend *L1cam* signaling and function. Indeed, in the past, modifier gene studies have made vital contributions to our understanding of signal transduction mechanisms, and they have revealed novel pathway components [78].

Acknowledgments We thank Shrikant Mane and Sheila Westman from the Yale Microarray Center, Jennifer Moran from the Mouse SNP Genotyping Service, Mutation Mapping and Developmental Analysis Project at Brigham and Women's Hospital, Genetics Division, Harvard Medical School, and Alison Brown from the Harvard Partners Center for Genetics and Genomics for SNP genotyping and evaluation. We also thank the Case Western Reserve Transgenic and Targeting Facility for their in vitro fertilization testing of *L1KO* mice. Our nomenclature for the *L1hydro1* locus was approved by the Mouse Genomic Nomenclature Committee of the Mouse Genome Informatics Resource, Jackson Laboratory. This work was supported by the Miami Project to Cure Paralysis and by National Institute of Health grants HD39884, EY05285, N01-NS-3-2351 and T32NS07459. V. Lemmon holds the Walter G. Ross Distinguished Chair in Developmental Neuroscience at the University of Miami.

References

1. Network NBDP (2007) Congenital malformations surveillance report: Birth defects surveillance data from selected states, 2000–2004. Birth Defects Research Part A 76:874–942
2. Persson EK, Anderson S, Wiklund LM, Uvebrant P (2007) Hydrocephalus in children born in 1999–2002: epidemiology, outcome and ophthalmological findings. Childs Nerv Syst 23:1111–1118
3. Jouet M, Rosenthal A, MacFarlane J, Kenwrick S, Donnai D (1993) A missense mutation confirms the L1 defect in X-linked hydrocephalus (HSAS). Nat Genet 4:331
4. Halliday J, Chow CW, Wallace D, Danks DM (1986) X linked hydrocephalus: a survey of a 20 year period in Victoria, Australia. J Med Genet 23:23–31
5. Vincent C, Kalatzis V, Compain S, Levilliers J, Slim R et al (1994) A proposed new contiguous gene syndrome on 8q consists of Branchio-Oto-Renal (BOR) syndrome, Duane syndrome, a dominant form of hydrocephalus and trapeze aplasia; implications for the mapping of the BOR gene. Hum Mol Genet 3:1859–1866
6. Dahme M, Bartsch U, Martini R, Anliker B, Schachner M et al (1997) Disruption of the mouse L1 gene leads to malformations of the nervous system. Nat Genet 17:346–349
7. Cohen NR, Taylor JS, Scott LB, Guillery RW, Soriano P et al (1998) Errors in corticospinal axon guidance in mice lacking the neural cell adhesion molecule L1. Curr Biol 8:26–33
8. Wang S, He F, Xiong W, Gu S, Liu H et al (2007) Polycomblike-2-deficient mice exhibit normal left-right asymmetry. Dev Dyn 236:853–861
9. Hirotsune S, Fleck MW, Gambello MJ, Bix GJ, Chen A et al (1998) Graded reduction of Pafah1b1 (Lis1) activity results in neuronal migration defects and early embryonic lethality. Nat Genet 19:333–339
10. Hong HK, Chakravarti A, Takahashi JS (2004) The gene for soluble N-ethylmaleimide sensitive factor attachment protein alpha is mutated in hydrocephaly with hop gait (hyh) mice. Proc Natl Acad Sci U S A 101:1748–1753
11. Chae TH, Kim S, Marz KE, Hanson PI, Walsh CA (2004) The hyh mutation uncovers roles for alpha Snap in apical protein localization and control of neural cell fate. Nat Genet 36:264–270
12. das Neves L, Duchala CS, Tolentino-Silva F, Haxhiu MA, Colmenares C et al (1999) Disruption of the murine nuclear factor I-A gene (Nfia) results in perinatal lethality, hydrocephalus, and agenesis of the corpus callosum. Proc Natl Acad Sci U S A 96:11946–11951
13. Zhang J, Williams MA, Rigamonti D (2006) Genetics of human hydrocephalus. J Neurol 253:1255–1266
14. Galbreath E, Kim SJ, Park K, Brenner M, Messing A (1995) Overexpression of TGF-beta 1 in the central nervous system of transgenic mice results in hydrocephalus. J Neuropathol Exp Neurol 54:339–349
15. Wyss-Coray T, Feng L, Masliah E, Ruppe MD, Lee HS et al (1995) Increased central nervous system production of extracellular matrix components and development of hydrocephalus in transgenic mice overexpressing transforming growth factor-beta 1. Am J Pathol 147:53–67
16. Zygourakis CC, Rosen GD (2003) Quantitative trait loci modulate ventricular size in the mouse brain. J Comp Neurol 461:362–369
17. Jones HC, Yehia B, Chen GF, Carter BJ (2004) Genetic analysis of inherited hydrocephalus in a rat model. Exp Neurol 190:79–90
18. Davy BE, Robinson ML (2003) Congenital hydrocephalus in hy3 mice is caused by a frameshift mutation in Hydin, a large novel gene. Hum Mol Genet 12:1163–1170
19. Lechtreck KF, Delmotte P, Robinson ML, Sanderson MJ, Witman GB (2008) Mutations in Hydin impair ciliary motility in mice. J Cell Biol 180:633–643
20. Ibanez-Tallon I, Gorokhova S, Heintz N (2002) Loss of function of axonemal dynein Mdnah5 causes primary ciliary dyskinesia and hydrocephalus. Hum Mol Genet 11:715–721
21. Obara T, Mangos S, Liu Y, Zhao J, Wiessner S et al (2006) Polycystin-2 immunolocalization and function in zebrafish. J Am Soc Nephrol 17:2706–2718
22. Pathak N, Obara T, Mangos S, Liu Y, Drummond IA (2007) The zebrafish fleer gene encodes an essential regulator of cilia tubulin polyglutamylation. Mol Biol Cell 18:4353–4364

23. Ferrante MI, Romio L, Castro S, Collins JE, Goulding DA et al (2009) Convergent extension movements and ciliary function are mediated by ofd1, a zebrafish orthologue of the human oral-facial-digital type 1 syndrome gene. Hum Mol Genet 18:289–303
24. Takeda Y, Asou H, Murakami Y, Miura M, Kobayashi M et al (1996) A nonneuronal isoform of cell adhesion molecule L1: tissue-specific expression and functional analysis. J Neurochem 66:2338–2349
25. Kamiguchi H, Lemmon V (1997) Neural cell adhesion molecule L1: signaling pathways and growth cone motility. J Neurosci Res 49:1–8
26. Esch T, Lemmon V, Banker G (2000) Differential effects of NgCAM and N-cadherin on the development of axons and dendrites by cultured hippocampal neurons. J Neurocytol 29:215–223
27. Lagenaur C, Lemmon V (1987) An L1-like molecule, the 8D9 antigen, is a potent substrate for neurite extension. Proc Natl Acad Sci U S A 84:7753–7757
28. Kunz S, Spirig M, Ginsburg C, Buchstaller A, Berger P et al (1998) Neurite fasciculation mediated by complexes of axonin-1 and Ng cell adhesion molecule. J Cell Biol 143:1673–1690
29. Stallcup WB, Beasley L (1985) Involvement of the nerve growth factor-inducible large external glycoprotein (NILE) in neurite fasciculation in primary cultures of rat brain. Proc Natl Acad Sci U S A 82:1276–1280
30. Itoh K, Fushiki S, Kamiguchi H, Arnold B, Altevogt P et al (2005) Disrupted Schwann cell-axon interactions in peripheral nerves of mice with altered L1-integrin interactions. Mol Cell Neurosci 30:624–629
31. Lindner J, Rathjen FG, Schachner M (1983) L1 mono- and polyclonal antibodies modify cell migration in early postnatal mouse cerebellum. Nature 305:427–430
32. Itoh K, Shimono K, Lemmon V (2005) Dephosphorylation and internalization of cell adhesion molecule L1 induced by theta burst stimulation in rat hippocampus. Mol Cell Neurosci 29:245–249
33. Nakamura Y, Tamura H, Horinouchi K, Shiosaka S (2006) Role of neuropsin in formation and maturation of Schaffer-collateral L1cam-immunoreactive synaptic boutons. J Cell Sci 119:1341–1349
34. Triana-Baltzer GB, Liu Z, Berg DK (2006) Pre- and postsynaptic actions of L1-CAM in nicotinic pathways. Mol Cell Neurosci 33:214–226
35. Lemmon V, Farr KL, Lagenaur C (1989) L1-mediated axon outgrowth occurs via a homophilic binding mechanism. Neuron 2:1597–1603
36. Castellani V, De Angelis E, Kenwrick S, Rougon G (2002) Cis and trans interactions of L1 with neuropilin-1 control axonal responses to semaphorin 3A. Embo J 21:6348–6357
37. Doherty P, Walsh FS (1996) CAM-FGF receptor interactions: a model for axonal growth. Mol Cell Neurosci 8:99–111
38. Kulahin N, Li S, Hinsby A, Kiselyov V, Berezin V et al (2008) Fibronectin type III (FN3) modules of the neuronal cell adhesion molecule L1 interact directly with the fibroblast growth factor (FGF) receptor. Mol Cell Neurosci 37:528–536
39. Schmid RS, Pruitt WM, Maness PF (2000) A MAP kinase-signaling pathway mediates neurite outgrowth on L1 and requires Src-dependent endocytosis. J Neurosci 20:4177–4188
40. Schaefer AW, Kamei Y, Kamiguchi H, Wong EV, Rapoport I et al (2002) L1 endocytosis is controlled by a phosphorylation-dephosphorylation cycle stimulated by outside-in signaling by L1. J Cell Biol 157:1223–1232
41. Schaefer AW, Kamiguchi H, Wong EV, Beach CM, Landreth G et al (1999) Activation of the MAPK signal cascade by the neural cell adhesion molecule L1 requires L1 internalization. J Biol Chem 274:37965–37973
42. Dickson TC, Mintz CD, Benson DL, Salton SR (2002) Functional binding interaction identified between the axonal CAM L1 and members of the ERM family. J Cell Biol 157:1105–1112
43. Cheng L, Itoh K, Lemmon V (2005) L1-mediated branching is regulated by two ezrin-radixin-moesin (ERM)-binding sites, the RSLE region and a novel juxtamembrane ERM-binding region. J Neurosci 25:395–403
44. Davis JQ, Bennett V (1994) Ankyrin binding activity shared by the neurofascin/L1/NrCAM family of nervous system cell adhesion molecules. J Biol Chem 269:27163–27166
45. Hortsch M, Nagaraj K, Godenschwege TA (2009) The interaction between L1-type proteins and ankyrins—a master switch for L1-type CAM function. Cell Mol Biol Lett 14:57–69
46. Cheng L, Lemmon S, Lemmon V (2005) RanBPM is an L1-interacting protein that regulates L1-mediated mitogen-activated protein kinase activation. J Neurochem 94:1102–1110
47. Yamasaki M, Thompson P, Lemmon V (1997) CRASH syndrome: mutations in L1CAM correlate with severity of the disease. Neuropediatrics 28:175–178
48. Kamiguchi H, Hlavin ML, Yamasaki M, Lemmon V (1998) Adhesion molecules and inherited diseases of the human nervous system. Annu Rev Neurosci 21:97–125
49. Fransen E, Van Camp G, D'Hooge R, Vits L, Willems PJ (1998) Genotype-phenotype correlation in L1 associated diseases. J Med Genet 35:399–404
50. Schrander-Stumpel C, Howeler C, Jones M, Sommer A, Stevens C et al (1995) Spectrum of X-linked hydrocephalus (HSAS), MASA syndrome, and complicated spastic paraplegia (SPG1): clinical review with six additional families. Am J Med Genet 57:107–116
51. Willems PJ, Brouwer OF, Dijkstra I, Wilmink J (1987) X-linked hydrocephalus. Am J Med Genet 27:921–928
52. Yamasaki M, Arita N, Hiraga S, Izumoto S, Morimoto K et al (1995) A clinical and neuroradiological study of X-linked hydrocephalus in Japan. J Neurosurg 83:50–55
53. Renier WO, Ter Haar BG, Slooff JL, Hustinx TW, Gabreels FJ (1982) X-linked congenital hydrocephalus. Clin Neurol Neurosurg 84:113–123
54. Boyd E, Schwartz CE, Schroer RJ, May MM, Shapiro SD et al (1993) Agenesis of the corpus callosum associated with MASA syndrome. Clin Dysmorphol 2:332–341
55. Fried K (1972) X-linked mental retardation and-or hydrocephalus. Clin Genet 3:258–263
56. Kaepernick L, Legius E, Higgins J, Kapur S (1994) Clinical aspects of the MASA syndrome in a large family, including expressing females. Clin Genet 45:181–185
57. Serville F, Lyonnet S, Pelet A, Reynaud M, Louail C et al (1992) X-linked hydrocephalus: clinical heterogeneity at a single gene locus. Eur J Pediatr 151:515–518
58. Fransen E, D'Hooge R, Van Camp G, Verhoye M, Sijbers J et al (1998) L1 knockout mice show dilated ventricles, vermis hypoplasia and impaired exploration patterns. Hum Mol Genet 7:999–1009
59. Rolf B, Kutsche M, Bartsch U (2001) Severe hydrocephalus in L1-deficient mice. Brain Res 891:247–252
60. Itoh K, Cheng L, Kamei Y, Fushiki S, Kamiguchi H et al (2004) Brain development in mice lacking L1-L1 homophilic adhesion. J Cell Biol 165:145–154
61. Hof PR, Young WG, Bloom FE, Belichenko PV, Celio MR (2000) Comparative cytoarchitectonic atlas of the C57BL/6 and 129/Sv mouse brains. Elsevier, New York
62. Abramoff MD, Magelhaes PJ, Ram SJ (2004) Image processing with ImageJ. Biophoton Int 11:36–42
63. Lorentzen JC, Glaser A, Jacobsson L, Galli J, Fakhrai-rad H et al (1998) Identification of rat susceptibility loci for adjuvant-oil-induced arthritis. Proc Natl Acad Sci U S A 95:6383–6387

64. Varga L, Muller G, Szabo G, Pinke O, Korom E et al (2003) Mapping modifiers affecting muscularity of the myostatin mutant (Mstn(Cmpt-dl1Abc)) compact mouse. Genetics 165:257–267
65. Broman KW, Wu H, Sen S, Churchill GA (2003) R/qtl: QTL mapping in experimental crosses. Bioinformatics 19:889–890
66. Broman KW, Sen S, Owens SE, Manichaikul A, Southard-Smith EM et al (2006) The X chromosome in quantitative trait locus mapping. Genetics 174:2151–2158
67. Zapala MA, Hovatta I, Ellison JA, Wodicka L, Del Rio JA et al (2005) Adult mouse brain gene expression patterns bear an embryologic imprint. Proc Natl Acad Sci U S A 102:10357–10362
68. Lander E, Kruglyak L (1995) Genetic dissection of complex traits: guidelines for interpreting and reporting linkage results. Nat Genet 11:241–247
69. Beck JA, Lloyd S, Hafezparast M, Lennon-Pierce M, Eppig JT et al (2000) Genealogies of mouse inbred strains. Nat Genet 24:23–25
70. Redzic ZB, Segal MB (2004) The structure of the choroid plexus and the physiology of the choroid plexus epithelium. Adv Drug Deliv Rev 56:1695–1716
71. Schwartz YB, Pirrotta V (2007) Polycomb silencing mechanisms and the management of genomic programmes. Nat Rev, Genet 8:9–22
72. Hu DD, Lin EC, Kovach NL, Hoyer JR, Smith JW (1995) A biochemical characterization of the binding of osteopontin to integrins alpha v beta 1 and alpha v beta 5. J Biol Chem 270:26232–26238
73. Wai PY, Kuo PC (2008) Osteopontin: regulation in tumor metastasis. Cancer Metastasis Rev 27:103–118
74. Gongidi V, Ring C, Moody M, Brekken R, Sage EH et al (2004) SPARC-like 1 regulates the terminal phase of radial glia-guided migration in the cerebral cortex. Neuron 41:57–69
75. Kim JM, Masai H (2004) Genetic dissection of mammalian Cdc7 kinase: cell cycle and developmental roles. Cell Cycle 3:300–304
76. Andres JL, Ronnstrand L, Cheifetz S, Massague J (1991) Purification of the transforming growth factor-beta (TGF-beta) binding proteoglycan betaglycan. J Biol Chem 266:23282–23287
77. Kirkbride KC, Townsend TA, Bruinsma MW, Barnett JV, Blobe GC (2008) Bone morphogenetic proteins signal through the transforming growth factor-beta type III receptor. J Biol Chem 283:7628–7637
78. St Johnston D (2002) The art and design of genetic screens: drosophila melanogaster. Nat Rev, Genet 3:176–188